Biosensors and Bioelectronics ■ (■■■■) ■■■–■■■

Contents lists available at ScienceDirect

Biosensors and Bioelectronics

journal homepage: www.elsevier.com/locate/bios

ZnO–CuO composite matrix based reagentless biosensor for detection of total cholesterol

Neha Batra [a], Monika Tomar [b], Vinay Gupta [a,*]

[a] Department of Physics and Astrophysics, University of Delhi, Delhi 110007, India
[b] Department of Physics, Miranda House, University of Delhi, Delhi 110007, India

ARTICLE INFO

Article history:
Received 27 May 2014
Received in revised form
2 August 2014
Accepted 18 August 2014

Keywords:
Reagentless
Total cholesterol
ZnO–CuO composite
Pulsed laser deposition

ABSTRACT

An efficient reagentless biosensor for determination of free cholesterol and total cholesterol has been realized using a ZnO–CuO composite matrix grown onto ITO coated corning glass substrates by pulsed laser deposition (PLD) technique. The inclusion of CuO in ZnO matrix successfully introduces redox property and provides enhanced electron communication features. The optimized ZnO–CuO composite matrix has been used for development of ChOx/(ZnO–CuO)/ITO/glass and (ChEt–ChOx)/(ZnO–CuO)/ITO/glass bioelectrodes used for selective detection of free and total cholesterol respectively in the range of 0.12–12.93 mM and 0.5–12 mM without using any external mediator. The fabricated biosensors exhibit high sensitivity of about 680 μA mM^{-1} cm^{-2} and 760 μA mM^{-1} cm^{-2} towards free cholesterol and total cholesterol respectively with response time of 5 s, along with high shelf life. The results are encouraging and show the promising application of the ZnO–CuO composite matrix for the realization of reagentless integrated implantable biosensor.

1. Introduction

Cholesterol is a vital component in cells and tissues of humans, playing a functional role in construction of cell membranes or serving as a biosynthetic precursor of bile acids, vitamin D, steroid hormones etc. It is produced by liver and circulates in blood, playing an important role in the brain, nervous and immune systems of humans (Parlak et al., 2013; Zhu et al., 2013). Despite the fact that cholesterol is a vital component of human mechanism its levels need a constant monitoring. The normal level of cholesterol being 3.1–6.7 mM, its elevated levels may lead to various disorders like heart diseases, coronary artery disease, arteriosclerosis, hypertension, cerebral thrombosis etc. while reduced levels lead to diseases such as hyperthyroidism, anemia malabsorption etc. (Cao et al., 2013). Extensive attempts have been made worldwide to develop highly selective and sensitive biosensors for the clinical diagnosis of cholesterol (Zhu et al., 2013; Cao et al., 2013). Zhu et al. (2013) have developed a biosensor based on direct electrochemistry of cholesterol oxidase immobilized on the gold nanoparticles-decorated multiwalled carbon nanotubes for detection of free cholesterol. The electrochemical biosensor for free cholesterol monitoring has been developed using multienzymatic electrode system with horseradish peroxidase (HRP) and cholesterol oxidase based on polymeric matrix (Bongiovanni et al., 2001). Although there are several reports in literature on the detection of cholesterol but demands external mediator in PBS buffer for redox reaction and are not suitable for realization of integrated biosensor. Recently Matharu et al. (2012) have developed a mediator free SAM based biosensor for detection of free and total cholesterol, but exhibit poor sensitivity. On the other hand the polymer based matrices are known to degrade with time whereas usage of mutienzymes leads to increase in the cost besides problem of leaching. Further most of the biosensors reported in literature were focused on detection of only free cholesterol. Thus it is very important to fabricate an efficient biosensor for reagentless detection of both free and total cholesterol with enhanced response characteristics.

ZnO (ZnO), a wide band gap semiconductor (~3.37 eV) with unique properties has potential for a variety of applications including piezoelectric devices, UV lasers, UV photodetectors, spintronics, gas sensors etc. (Yadav et al., 2010). The good biocompatibility, high chemical stability, good electrochemical properties and, high isoelectric point (IEP 9.5) of ZnO makes it suitable for biosensing applications as well (Saha and Gupta, 2011a). ZnO matrix has been exploited for detection of wide variety of biomolecules including glucose (Saha and Gupta, 2011a), cholesterol (Solanki et al., 2009), urea (Ali et al., 2009), Phenol (Gu et al., 2009), H_2O_2 (Zhu et al., 2007), DNA (Wang et al., 2006) etc. with high sensitivity and stability. However, ZnO does not possess a redox couple of its own which necessitates the use of external

* Corresponding author. Tel.: +91 9811563101.
E-mail addresses: drguptavinay@gmail.com, vgupta@physics.du.ac.in (V. Gupta).

http://dx.doi.org/10.1016/j.bios.2014.08.029
0956-5663/

electroactive mediators for electron transfer between the enzyme and the electrode (Saha and Gupta, 2011b). Several efforts have been made towards incorporation of redox property into the ZnO based matrices. The redox property in ZnO matrix has been introduced using implantation of foreign elements having multivalence state and reagentless detection of glucose is demonstrated with good stability (Saha and Gupta, 2011b). ZnO thin film are also doped with Fe; however CV spectra were distorted and the sensing response characteristics were poor (Saha and Gupta, 2011b).

Alternatively, CuO has also been exploited for development of reagentless biosensors (Jindal et al., 2012). Although the sensitivity of CuO based biosensors were very high, but stability and shelf life becomes very poor (Jindal et al., 2012). The composite of ZnO with CuO may result in better matrix with improved stability for development of reagentless biosensor with enhanced response. In the present work effort has been made to fabricate the composite matrix of ZnO and CuO using pulsed laser deposition (PLD) technique and detection of both free and total cholesterol are demonstrated successfully with enhanced response characteristics without using any external mediator.

2. Experimental

2.1. Reagents and solutions

Cholesterol oxidase (ChOx) from Streptomyces species, cholesterol esterase (ChEt) from *Pseudomonas* species, Triton X-100, polyoxyethylene-9-lauryl ether, cholesterol and cholesteryl oleate were procured from Sigma-Aldrich. Sodium phosphate monobasic anhydrous and sodium phosphate dibasic dihydrate were obtained from Sisco chemical, India. ZnO powder (99.9% purity) was acquired from Merck and Co. All the Chemicals were used without further purification. Deionized water (resistivity 18.2 MΩ cm) was used in the preparation of aqueous solutions. Phosphate buffer saline (PBS) 50 mM, pH 7.0 (0.9% NaCl) solution was prepared by mixing 39 ml of 0.2 M monobasic sodium phosphate solution with 61 ml of 0.2 M dibasic sodium phosphate solution and then adding 0.9% NaCl to the solution. ChEt and ChOx (1 mg ml^{-1}) solution were freshly prepared in PBS buffer of pH 7.0. The stock solution of cholesterol is prepared in 10% Triton X-100, and Stock solution of cholesteryl oleate was prepared in polyoxyethylene-9-lauryl ether (since both the compounds are water insoluble) and stored at 4 °C.

2.2. Growth of ZnO–CuO composite thin film

The processing parameters that play important role during the deposition process of oxide thin films in PLD technique include background gas, growth pressure, substrate temperature, laser energy density, target to substrate distance and the pulse repetition rate. Oxide thin films grown using PLD technique at low oxygen pressure are reported to be oxygen deficient, and a moderate background oxygen pressure becomes necessary to maintain the equilibrium composition of the target in the deposited thin films (Kim and Lee, 2004). A high substrate temperature favours defect free growth of ZnO crystallites due to full oxidization of zinc atoms and optimum surface diffusion of the ablated species, whereas a low substrate temperature results in the growth of a disordered or poorly crystallized structure (Tsoutsouva et al., 2011).

The particular deposition conditions in the present work were selected on basis of optimization of deposition parameters. Firstly the deposition pressure was varied from 50 to 500 mT while keeping the other parameters (such as substrate temperature, target–substrate distance etc.) fixed. It was found that the matrix deposited at 100 mT was giving best CV response both in terms of maximum peak oxidation current and minimum peak to peak separation between the oxidation and reduction peaks. Subsequently the deposition pressure was kept fixed at 100 mT and substrate temperature was varied from room temperature to 400 °C. It was found that a substrate temperature of 300 °C was optimum to prepare a matrix with good CV response and stable characteristics.

Thin films of ZnO–CuO composites were deposited onto the ITO coated corning glass (ITO/glass) platform by pulsed laser deposition (PLD) technique at an oxygen pressure of 100 mT and substrate temperature of 300 °C. The fourth harmonic of Nd:YAG laser (λ=266 nm) at a pulse rate of 10 Hz is used to ablate the ZnO and Cu targets of one inch diameter sequentially. ZnO ceramic target was prepared by pressing ZnO powder (99.99% pure) followed by sintering at 1000 °C for 4 h. The thickness of each layer (ZnO or CuO) in the composite structure was controlled from the number of shots of the laser pulses used to strike the respective targets. In the present work 10% content of CuO in the composite matrix of ZnO–CuO was used for sensing purposes. The content of CuO was optimized in preliminary set of experiments to yield a cyclic voltammogram with well defined oxidation and reduction peaks in absence of any external mediator. The composite matrix was annealed in air at 300 °C for 2 h to stabilize the prepared sensor. The total thickness of the composite thin film was fixed to be 120 nm. The prepared composite electrode ((ZnO–CuO)/ITO/glass) has been studied for its structural, optical, electrical and electrochemical properties. For comparison, pure ZnO thin film (120 nm) was also deposited under identical growth condition.

The crystalline structure of composite thin films was identified by X-ray Diffraction (XRD) technique (Bruker D8). Optical properties of the films and photometric assay of the bioelectrodes were studied using UV–visible spectrophotometer (Perkin Elmer: lambda 35). To study the electrochemical properties of the bioelectrode, cyclic voltammetric measurements were carried out using a Potentiostat/Galvanostat (Gamry Inc., Reference 600) under a three-electrode electrochemical cell configuration with Ag/AgCl serving as reference electrode, platinum (Pt) foil as counter electrode and CuO–ZnO/ITO/glass (or ZnO/ITO/glass) as working electrode.

2.3. Preparation of bioelectrode

The 10 μl of the freshly prepared ChOx solution (1 mg/ml in PBS solution) is spread on the surface of (ZnO–CuO)/ITO/glass electrode to immobilize the ChOx electrostatically via physical adsorption technique and ChOx/(ZnO–CuO)/ITO/glass bioelectrode is prepared for detection of free cholesterol. For the estimation of total cholesterol, both ChEt (IEP=4.5) (Kontkanen et al., 2006) and ChOx (IEP=4.7) have been co-immobilized on the surface of ZnO–CuO composite matrix by physical adsorption technique. 10 μl of ChEt (1 mg/ml) and ChOx (1 mg/ml) solution (1:1) is uniformly spread onto the surface of composite matrix and dried at room temperature for an hour. The bioelectrodes are kept overnight at 4 °C and subsequently washed with buffer solution. The prepared bioelectrodes ((ChEt–ChOx)/(ZnO–CuO)/ITO/glass) and (ChOx/(ZnO–CuO)/ITO/glass) are stored at 4 °C when not in use.

3. Results and discussion

3.1. Structural studies

The as-deposited thin film of pure ZnO and ZnO–CuO composite were found to be transparent and strongly adherent to the surface of ITO/glass platform. Fig. 1(a) shows the XRD pattern of

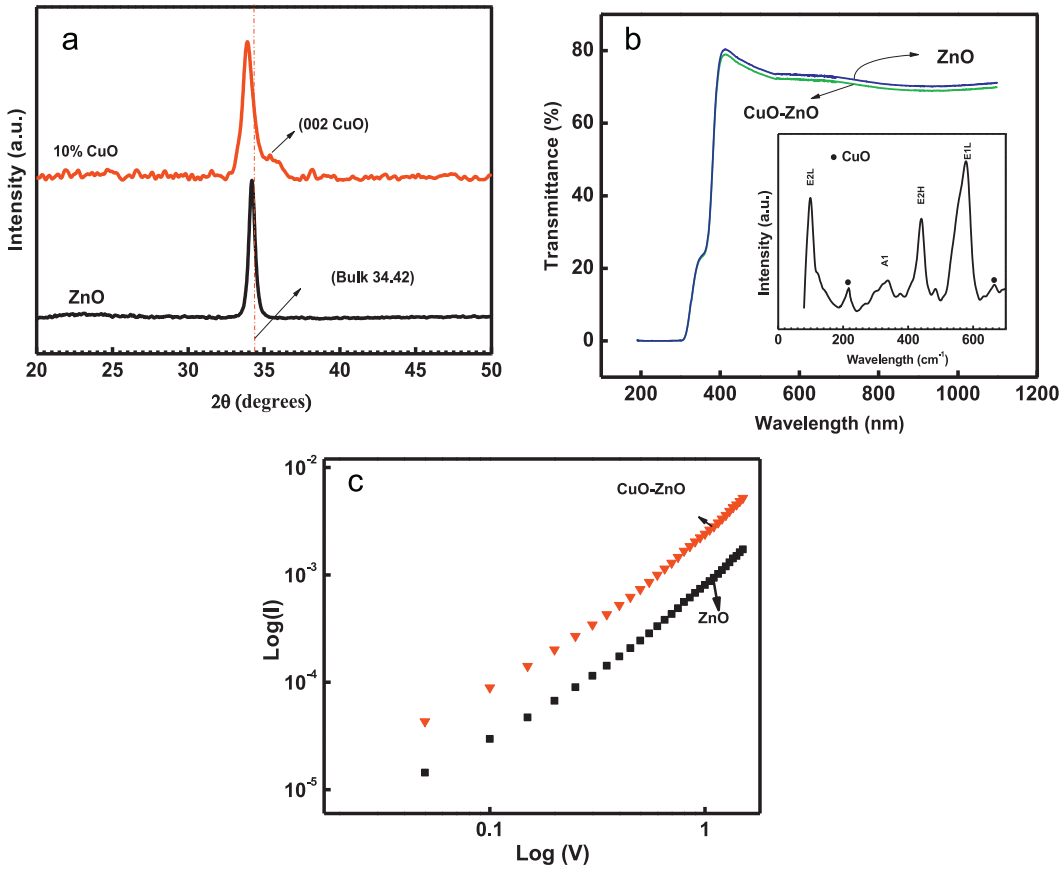

Fig. 1. (a) XRD spectra of ZnO and (ZnO–CuO) composite thin films. (b) UV–visible transmission spectra of ZnO and ZnO–CuO composite thin films. Inset shows Raman spectra of (ZnO–CuO) composite thin film. (c) *I–V* characteristics of ZnO and composite ZnO thin films.

both the ZnO and ZnO–CuO composite thin films. Only one peak corresponding to (002) plane of the wurtzite structure of ZnO was observed in the XRD pattern of both the samples, indicating the growth of highly preferred oriented thin films with the *c*-axis normal to substrate. A small peak at $2\theta \approx 35.4^{\circ}$ corresponding to the (002) plane of CuO is also seen in composite thin film sample indicating the formation of ZnO–CuO composite matrix (Jindal et al., 2012). The FWHM of (002) XRD peak of ZnO was found to increase upon incorporation of CuO in composite matrix (Fig. 1(a)). Grain size as calculated using Scherrer's formula from the dominant (002) peak is found to decrease from 24 nm to 15 nm on incorporation of CuO in the ZnO matrix. The lower size grains of ZnO–CuO composite matrix are beneficial for efficient loading of enzyme as it provides enhanced surface to volume ratio. The values of lattice constant '*c*', grain size and stress estimated from XRD data are tabulated in Supplementary Table S1. The (002) peak of wurtzite ZnO structure was seen to shift towards lower angles upon incorporation of CuO (Fig. 1(a)) leading to lattice expansion along c-axis and resulting in the presence of tensile stress in the composite matrix.

3.2. Optical property

For optical studies both ZnO and ZnO–CuO composite thin films were prepared on the glass slides under identical deposition conditions. Fig. 1(b) shows the UV–visible transmission spectra of the ZnO and ZnO–CuO composite thin films. It may be seen from Fig. 1(b) that both matrices are highly transparent (> 70%) in the visible region (Fig. 1(b)). The onset of sharp fundamental absorption edge corresponding to inter-band band transition is observed for both the prepared samples at around 380 nm (Fig. 1(b)). The value of the optical bandgap (E_g) evaluated from the Tauc plot was found to decrease from 3.25 eV to 3.20 eV with the incorporation of CuO in the ZnO matrix. The lower value of band gap for ZnO–CuO composite matrix is attributed to the fact that CuO has relatively low value of bandgap (1.2–1.9 eV) in comparison to that of ZnO (3.37 eV) (Jindal et al., 2012).

3.3. Raman spectroscopy study

Room temperature Raman spectra obtained in back scattering configuration for ZnO–CuO composite thin film is shown in the inset of Fig. 1(b). Well defined and sharp Raman modes were observed at 90, 331, 433 and 573 cm^{-1}. The peaks observed at 90 cm^{-1} and 433 cm^{-1} are the characteristic phonon modes of ZnO wurtzite phase corresponding to the E_2 (low) and E_2 (high) respectively (Gupta et al., 2006). The phonon modes observed at 331 cm^{-1} and 573 cm^{-1} correspond to A_1 and E_1 (LO) modes of ZnO respectively (Yadav and Gupta, 2012). The appearance of E_1 (LO) mode is due to the presence of native defects in the matrix such as oxygen interstitials, zinc vacancies etc. and are expected to yield the better electron communication properties (Saha and Gupta, 2011a). It is also interesting to observe the onset of well-defined phonon peaks at 216 cm^{-1} and 625 cm^{-1} (inset of Fig. 1 (b)) which are attributed to A_g and $B_g^{(2)}$ modes corresponding to the vibrations of oxygen atoms in the CuO matrix (Zhu et al., 2006). The obtained results confirm formation of ZnO–CuO composite matrix.

Please cite this article as: Batra, N., et al., Biosensors and Bioelectronics (2014), http://dx.doi.org/10.1016/j.bios.2014.08.029

3.4. Electrical property

The current–voltage (*I–V*) characteristics of the ZnO and ZnO–CuO composite matrices were studied in metal–semiconductor–metal (MSM) configuration using Pt/Ti as the bottom metal electrode and circular Pt dots (600 μm diameter) as top metal electrodes. The respective thin film matrices were deposited under the identical growth conditions on the Pt/Ti coated glass slides. The Pt thin film of 100 nm thickness was deposited on glass slide by rf sputtering technique using a 3 in. diameter metal target of Pt (99.99% pure) in 100% Ar ambient and with a rf power of 100 W. A buffer layer of Ti (~10 nm) was deposited prior to Pt coating under similar growth condition to improve the adhesion of Pt on glass slide. Fig. 1(c) shows the room temperature current–voltage (*I–V*) curves obtained for both ZnO and ZnO–CuO composite matrices. The current was found to increase with increasing applied voltage (Fig. 1(c)) for both the samples, and the observed variation is in accordance with $I \alpha V^n$, where n is an exponent. The value of n was found to be close to 'one' in the lower bias (< 0.8 V) range, indicating the ohmic nature of the prepared electrodes. However, the current shows a rapid increase at higher applied bias (> 0.8 V) with $n > 1.0$ and may be attributed to the space charge limited conduction mechanism. It may also be noted from Fig. 1 (c) that the value of current at a fixed bias is higher for ZnO–CuO composite matrix in comparison to that of pure ZnO matrix, indicating improvement in the electrical property of composite matrix with incorporation of CuO. The room temperature value of dc conductivity estimated for ZnO and ZnO–CuO composite matrices are found to be about $1.95 \times 10^{-6}\ \Omega^{-1}\ cm^{-1}$ and $4.8 \times 10^{-6}\ \Omega^{-1}\ cm^{-1}$ respectively. The observed modulation in conductivity is due the presence of CuO having low band gap (1.2 eV) and the participation of holes in the conduction process increases the conductivity.

3.5. Electrochemical property

Cyclic voltammetry is often the first experiment performed in an electrochemical study of a compound, a biological material, or an electrode surface. The effectiveness of CV results from its capability for rapidly observing the redox behavior over a wide potential range.

The CV spectra in the present study was recorded with sweeping the applied potential over a range from – 0.5 V to +0.3 V and back. In the forward scan, when the potential is sufficiently positive to oxidize Cu^{1+} to Cu^{2+} in the composite matrix oxidation current starts flowing. The oxidation current increases continuously with applied potential till a peak value occurs, and thereafter a decrease in current in observed since the composite matrix is now depleted of Cu^{1+} species. During reverse scan the potential is still sufficient for oxidation and current flows continuously. When the potential becomes sufficiently low, the opposite process starts and the scan is completed in reverse direction. Along with redox reaction diffusion from bulk solution also contributes to the current. The characteristic of a CV spectra are the oxidation and reduction peaks corresponding to the redox species present in the working electrode. The observed well defined redox peaks for ZnO–CuO composite matrix in a mediator-free PBS buffer is attributed to the shuttling of electrons in the matrix from Cu^{1+} to Cu^{2+} and vice-versa.

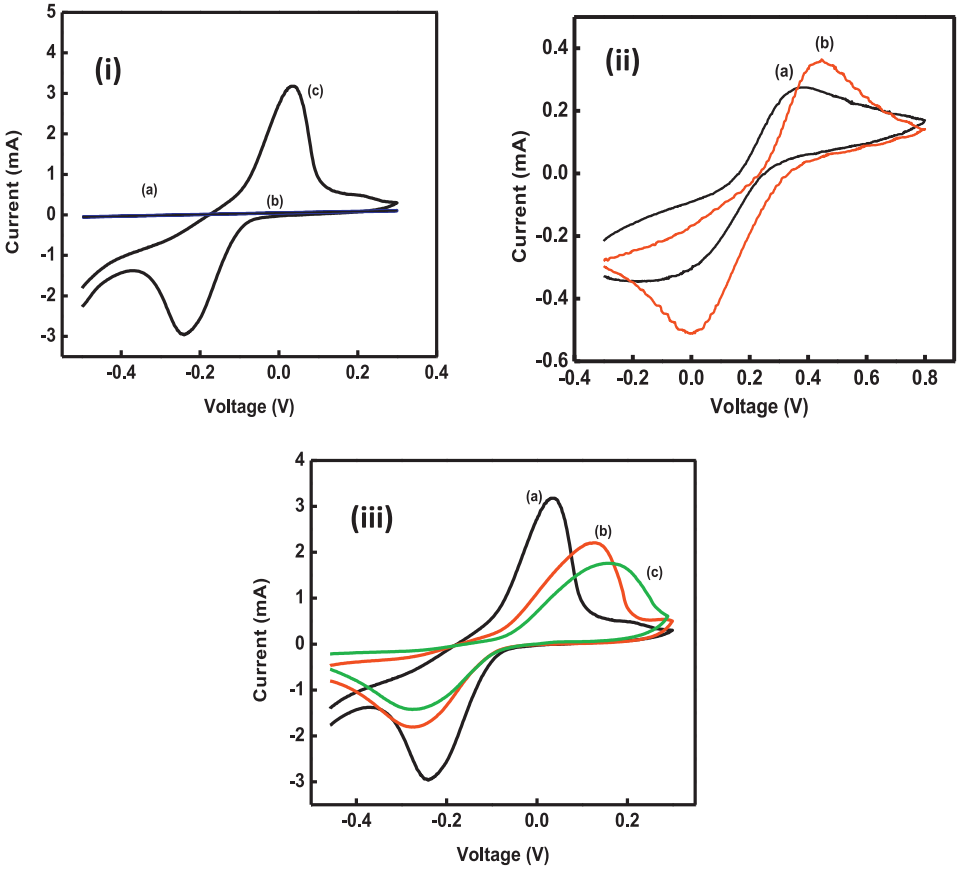

Fig. 2. (i) CV response of (a) ITO/glass and (b) ZnO/ITO/glass electrode and ZnO–CuO/ITO/glass electrode in PBS. (ii) CV response of (a) ITO/glass and (b) ZnO/ITO/glass electrode in PBS containing mediator. (iii) CV response of (a) ZnO–CuO/ITO/glass electrode, (b) ChOx/ZnO–CuO/ITO/glass bioelectrode and (c) (ChEt–ChOx)/ZnO–CuO/ITO/glass bioelectrodes in PBS.

Please cite this article as: Batra, N., et al., Biosensors and Bioelectronics (2014), http://dx.doi.org/10.1016/j.bios.2014.08.029

The cyclic voltammetry (CV) spectra for ITO/glass, ZnO/ITO/glass electrode and ZnO–CuO/ITO/glass electrode, were obtained using a three electrode cell, in the PBS buffer without using any external mediator and are shown in Fig. 2(i). It can be seen from Fig. 2(i) that both ITO/glass and ZnO/ITO/glass electrodes exhibit very low current and no redox peaks could be observed in the respective CV spectra. This is because of the fact that both ZnO and ITO do not possess any redox couple. For comparison purposes CV of the ITO/glass substrate, ZnO/ITO/glass electrode have been recorded in PBS solution containing 5 mM $K_3[Fe(CN)_6]$ as mediator are shown in Fig. 2(ii). Clear redox peaks are visible due to the presence of mediator. The peaks vanish in the case mediator is not used (Fig. 2(i)). However, (ZnO–CuO)/ITO/glass electrode shows a well-defined CV spectra (Fig. 2(i)) having a sharp oxidation peak with a high peak oxidation current (I_{po}) of about 3.21 mA. The observed well defined redox peaks for ZnO–CuO composite matrix in a mediator-free PBS buffer is attributed to the shuttling of electrons in the matrix from Cu^{1+} to Cu^{2+} and vice-versa (Jindal et al., 2012). The high value of I_{po} is due to enhanced electron communication feature of the prepared composite matrix. The oxidation peak for ZnO–CuO composite matrix is seen to occur at $V < 0.1$ V, and hence is attractive for possible negligible interference from other biomolecules present in the human serum while detection of cholesterol. Thus ZnO–CuO composite matrix having 10% CuO and 90% ZnO content is a suitable matrix for realization of an efficient reagentless and selective biosensor.

3.6. FTIR studies

For FTIR studies, ZnO–CuO composite film was deposited on Si wafer and the obtained FTIR spectra in transmission mode is shown in Fig. 3. The FTIR spectra of composite film (curve a) shows absorption bands at around 407 and 564 cm^{-1} which are attributed to E_1 (TO) and A_1 (LO) bending vibrations of ZnO respectively (Zerdali et al., 2006; Wei et al., 2009). The absorption band at 610 cm^{-1} is the local vibration in crystal lattice of Si wafer (Wei et al., 2009). In addition, a band is seen at 480 cm^{-1}, corresponding to Cu–O bond (Jindal et al., 2012), which confirms the formation of ZnO–CuO composite thin film.

The absorption bands corresponding to ZnO at 564 cm^{-1} and CuO at 480 cm^{-1} respectively is seen to shift to 547 cm^{-1} and 496 cm^{-1} upon immobilization of ChOx, on the surface of composite matrix (Fig. 3, curve b). The obtained results indicate that the phonon vibrations in ZnO–CuO matrix get disturbed due to electrostatic interaction with the enzyme molecules (Solanki et al., 2009; Singh et al., 2007; Jindal et al., 2012). FTIR spectra of ChOx/(ZnO–CuO)/Si bioelectode exhibits additional bands at 1005, 1451, 1643 and 3300 cm^{-1} (Fig. 3, curve b). The band at 1005 cm^{-1} is assigned to C–O stretching mode due to amide band in immobilized protein (Solanki et al., 2009), 1451 cm^{-1} corresponding to C–N axial deformation (amine group band), 1643 cm^{-1} corresponding to carbonyl stretch amide I and a broad band at 3300 cm^{-1} corresponding to amide B of the enzyme (Matharu

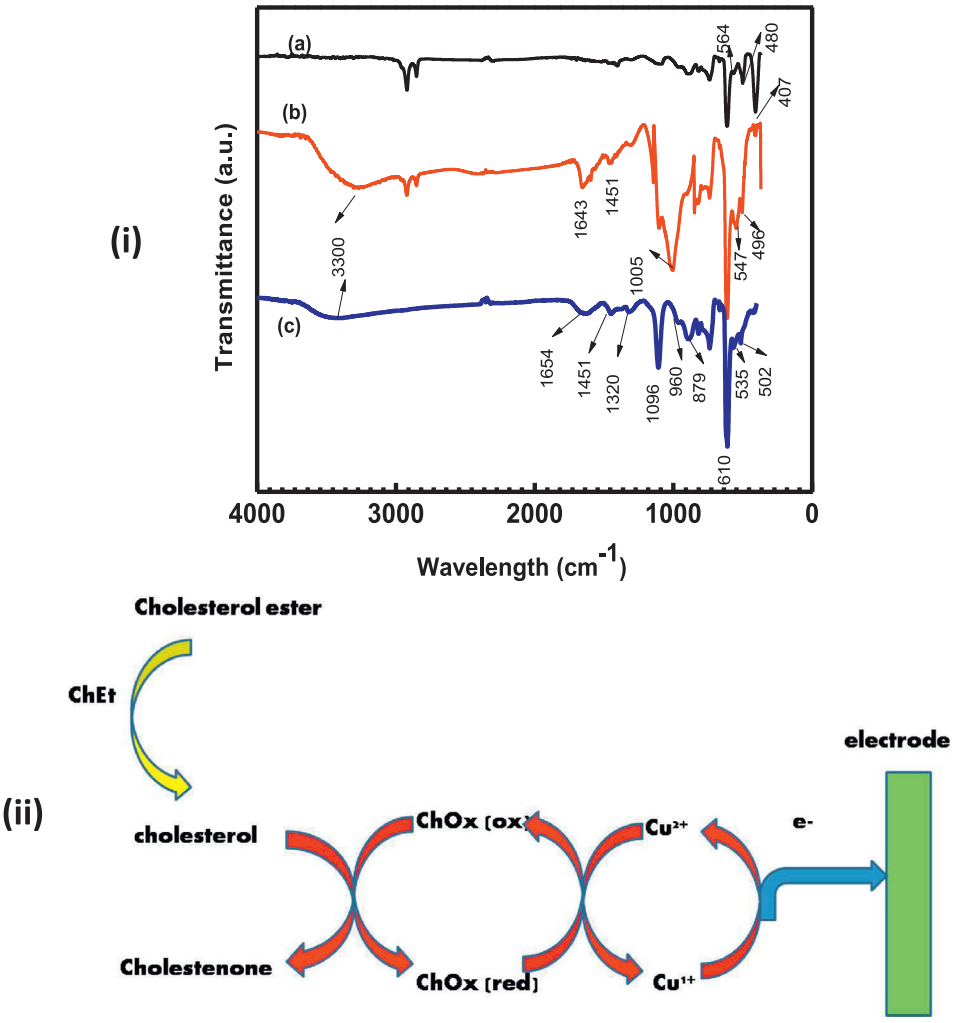

Fig. 3. (i) FTIR studies (ZnO–CuO)/Si,ChOx/(ZnO–CuO)/Si and (ChEt–ChOx)/ (ZnO–CuO)/Si. (ii) Schematic of the reaction occurring at the bioelectrode surface.

Please cite this article as: Batra, N., et al., Biosensors and Bioelectronics (2014), http://dx.doi.org/10.1016/j.bios.2014.08.029

et al., 2007). These results indicate the successful immobilization of ChOx over the surface of ZnO–CuO composite matrix.

Upon immobilization of both ChEt and ChOx the 564 cm^{-1} (due to ZnO) is further seen to shift to 535 cm^{-1} and band at 480 cm^{-1} (due to CuO) is seen to shift at 502 cm^{-1} (curve c). The results indicate the electrostatic interaction between the immobilized enzymes and the underneath composite matrix. In addition to modes exhibited by ChOx/ZnO–CuO/Si bioelectrode, FTIR spectra (Fig. 3, curve c) of (ChEt–ChOx)/(ZnO–CuO)/Si exhibits absorption bands at 879 cm^{-1} and 960 cm^{-1} assigned to stretching and bending vibrations respectively associated with C–N linkage, 1451 and 1320 cm^{-1} corresponding to carbonyl stretch amide I and II respectively confirming the co-immobilization of both ChOx and ChEt enzymes on the surface of composite matrix.

3.7. CV studies of bioelectrode

CV curves obtained for (ZnO–CuO)/ITO/glass electrode, ChOx/(ZnO–CuO)/ITO/glass and (ChEt–ChOx)/(ZnO–CuO)/ITO/glass bioelectrodes are shown in Fig. 2(iii). For comparison, the CV curves for ITO/glass and ZnO/ITO/glass electrodes are also shown in Fig. 2(i). Since ITO and ZnO does not possess the redox couple of their own, the CV spectra of ITO/glass electrode and ZnO/ITO/glass electrode (Fig. 2(i)) does not show any redox peak in the measured potential range in the PBS solution having no external mediator. However, the CV spectra of (ZnO–CuO)/ITO/glass electrode (Fig. 2(iii), curve a) showed a well-defined redox peaks having peak oxidation current $I_{po} \approx 3.2$ mA. It may be seen from Fig. 2(iii) that, the immobilization of ChOx over the (ZnO–CuO)/ITO/glass electrode (curve b) results in a decrease in the value of I_{po} from 3.2 to 2.3 mA, which further drops to 1.8 mA (curve c) upon immobilization of bienzymes (ChOx and ChEt). The observed reduction in I_{po} is indicative of the fact that some insulating moiety (biomolecules) has been immobilized on the working electrode that hinders the flow of charge carriers. Furthermore, it may also be seen from Fig. 2(iii) that the immobilization of enzymes increases the peak to peak separation between the oxidation and reduction peaks and is due to some voltage drop across the macro-molecules of insulating enzymes.

3.8. Effect of pH

In the present work, pH of buffer solution was varied with ZnO–CuO matrix (without immobilization of enzymes) as the working electrode. It was found that there was no change in peak oxidation current when the pH of the buffer solution was varied from 6 to 7.4, however a slight drop in current at pH 7.9 was observed. This drop in current is however within permissible limits of error. Hence it may be concluded that changes in pH of buffer solution do not affect CV spectra of the composite matrix.

Another experiment was performed in which effect of pH of the PBS buffer solution on the activity of prepared both bioelectrodes (ChOx/(ZnO–CuO)/ITO/glass and (ChET–ChOx/(ZnO–CuO)/ITO/glass)) was studied keeping the temperature fixed at 25 °C. Peak oxidation current in the CV of both the bioelectrode was recorded by varying the pH of buffer solution from 6.0 to 7.9. The peak oxidation current was found to be maximum at a pH of 7.0 and reduces on either increasing or decreasing the pH value, thus confirming enhanced bio-activity of the biomolecule at pH 7.0. As a result, pH of buffer solution was kept fixed at 7.0 throughout the experiments in the present work.

3.9. Amperometric biosensing response

The biosensing response of ChOx/(ZnO–CuO)/ITO/glass and (ChEt–ChOx)/((ZnO–CuO))/ITO/glass bioelectrodes towards free

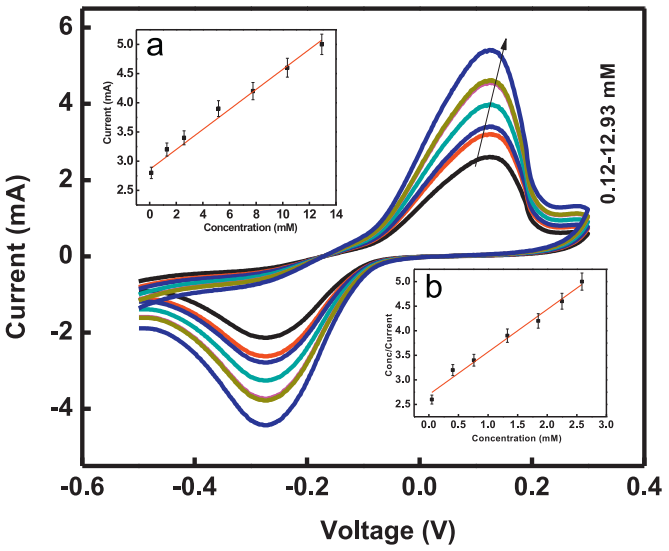

Fig. 4. CV response of ChOx/(ZnO–CuO)/ITO/glass bioelectrode with change in cholesterol concentration. Inset shows (a) Variation of peak oxidation current as a function of cholesterol concentration and (b) Hanes plot to calculate the Michaelis Menten kinetic parameter.

cholesterol and total cholesterol respectively have been carried out using CV measurements. CV scans have been taken in PBS solution (50 mM, pH 7, 0.9% NaCl) containing free cholesterol and total cholesterol in varying concentration for the respective bioelectrodes and without using any external mediator. The peak current, I_{po} is found to increase continuously with increasing the concentration of both analytes, free cholesterol (Fig. 4) and total cholesterol (Fig. 5). It may be seen from inset (a) of Figs. 4 and 5 that the value of I_{po} increases linearly with increase in concentration of free cholesterol and total cholesterol respectively from 0.12 to 12.93 mM and from 0.5 to 12 mM for the ChOx/(ZnO–CuO)/ITO/glass and ChOx–ChEt/(ZnO–CuO)/ITO/glass bioelectrodes respectively. To further improve the linear detection range of the biosensor, epitaxial growth of matrix is needed which demands the expensive single crystals with lattice matching. The imprecision of the sensors could be enhanced by using multipoint

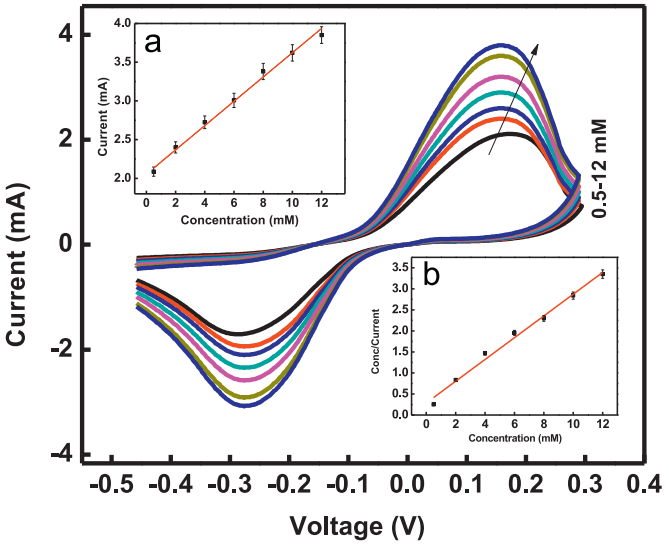

Fig. 5. CV response of ChEt–ChOx/ZnO–CuO/ITO/glass bioelectrode with change in the concentration of total cholesterol. Inset shows (a) Variation of peak oxidation current with total cholesterol concentration and (b) Hanes plot to calculate the Michaelis Menten kinetic parameter.

calibration of the sensor with reduced step size over the detection range.

The sensitivities of ChOx/ZnO–CuO/ITO/glass and (ChEt–ChOx)/ZnO–CuO/ITO/glass bioelectrodes as calculated from the respective calibration curves (inset b of Figs. 4 and 5) are found to be about 680 $\mu A\ mM^{-1}\ cm^{-2}$ and 760 $\mu A\ mM^{-1}\ cm^{-2}$, respectively. The sensitivity obtained in the present case for the composite (ZnO–CuO) matrix is much higher than the corresponding values reported in literature. Umar et al. (2009) reported a sensitivity of 61.7 $\mu A\ mM^{-1}\ cm^{-2}$ for ZnO based matrix for cholesterol detection. Ahmadalinezhad and Chen (2011) reported a sensitivity of 29.33 $\mu A\ mM^{-1}\ cm^{-2}$ for total cholesterol using nanoporous gold matrix. The higher sensitivity obtained in present case may be attributed to efficient and enhanced electron communication feature of the fabricated ZnO–CuO composite matrix. Furthermore, absence of any external mediator in the electrolyte solution is an added advantage compared to earlier reports on total cholesterol detection using metal or metal oxide matrices (Ahmadalinezhad and Chen, 2011).

The control experiment was performed in order to confirm that the immobilized enzyme (ChOx, or ChEt–ChOx) catalyzes the biochemical process with analyte and was responsible for the observed increase in peak oxidation current in CV spectra with analyte concentration. In this control experiment sensing response for cholesterol and total cholesterol respectively was studied without immobilization of the respective enzymes on the surface of (ZnO–CuO)/ITO/glass electrode. The control experiment revealed that there was no increase in oxidation and reduction currents in the CV response with increase in concentration of cholesterol and total cholesterol respectively. Thus, the performed control experiment confirmed that the increase in peak oxidation current observed in CV spectra for both bioelectrodes with varying concentration of cholesterol and total cholesterol respectively is only due to the biochemical reaction taking place in presence of immobilized ChOx and ChEt–ChOx respectively.

ChOx catalyzes the oxidation of cholesterol, while ChEt catalyzes the hydrolysis of esterified cholesterol, which is important for determination of total cholesterol. These enzymes help in monitoring both native and esterified cholesterol levels. The schematic of reaction occurring at the bioelectrode is shown in Fig. 3(ii). The cholesterol estimation is based on

$$\text{Cholesteryl esters} + H_2O \xrightarrow{\text{ChEt}} \text{Cholesterol} + \text{fatty acids}$$

$$\text{Cholesterol} + O_2 \xrightarrow{\text{ChOx}} 5\text{Cholest-3-one} + H_2O_2 \xrightarrow{\text{Isomerization}} 4\text{Cholest-3-one} + H_2O_2$$

ChEt converts cholesterol ester to free cholesterol. ChOx catalyses the oxidation of free cholesterol to cholestenone and in the process itself gets reduced. The reduced form of enzyme is inactive and needs to be reoxidized for further activity. Cu present in the composite ZnO–CuO matrix undergoes a change in oxidation state from Cu^{2+} to Cu^{1+} and in the process aids the reoxidation of enzyme. Thus the enzyme regains its enzymatic activity. Subsequently oxidation of Cu^{2+} to Cu^{1+} occurs via electron transfer to the electrode through the composite matrix, thus leading to increase in peak oxidation current. This increase in current is directly related to the concentration of analyte (cholesterol).

Thus sensing mechanism for both free cholesterol and total cholesterol is similar except that the ChEt hydrolysis the cholesterol esters to free cholesterol. The response time of the bioelectrode calculated by taking CV response at different time delays, is found to be relatively fast (5 s) and is because of the fast electron communication feature of the ZnO–CuO composite matrix. Due to large surface area of the ZnO–CuO composite matrix, large no. of biomolecules get attached to the surface due to the large surface to volume ratio provided by this electrode, thus the ChOx and (ChEt–ChOx) attached to the surface of ZnO–CuO matrix facilitates the fast electron transfer resulting in increased sensitivity.

The sensitivity of an enzymatic electrochemical biosensor relies on shuttling of the electrons, generated in the biochemical reaction, from the redox center of the enzyme (ChOx) to the electrode via ZnO thin film matrix. ZnO in lack of any redox couple of its own is unable to aid in this electron transfer process.

Copper oxide (CuO), a p-type semiconductor rmetal oxide with a narrow bandgap (1.2 eV) has been of immense interest as a matrix in biosensors recently owing to its non-toxicity, good electrochemical activity, high isoelectric point (IEP_9.5) and the possibility of redox reaction due to multiple valence states exhibited by Cu. Thus addition of CuO solves the issue, as Cu is able to change reversibly from Cu^{1+} to Cu^{2+} and vice versa. The peak oxidation current obtained in CV analysis of ZnO–CuO composite is much higher ($\sim$2.1 mA) compared to that exhibited by pure ZnO in presence of mediator ($\sim$0.3 mA). The high peak current could be attributed to the incorporation of p-type CuO in the composite matrix with provides good electron transfer property (Tyagi et al., 2012). Thus presence of CuO with ZnO in the composite matrix enhances the sensitivity of cholesterol biosensor. However the shelf life of biosensors is relatively higher due to presence of ZnO in the composite matrix. The results obtained in the present work clearly suggest that the composite matrix of CuO with ZnO solves the problem of requirement of external mediator in the PBS solution by introducing the redox property in the electrode itself while exhibiting the enhanced sensitivity and good life time of the bioelectrode.

The Michaelis–Menten kinetic parameter (K_m) of enzymatic reaction has been estimated using Hanes plot i. e. graph between the analyte concentration and the ratio of analyte concentration/I_{po}. The Hanes plots for the ChOx/(ZnO–CuO)/ITO/glass and ChOx–ChEt/(ZnO–CuO)/ITO/glass bioelectrode respectively are shown in inset (b) of Figs. 4 and 5. The estimated value of K_m for ChOx/(ZnO–CuO)/ITO/glass and (ChEt–ChOx)/(ZnO–CuO)/ITO/glass bioelectrodes are about 3.13 mM and 1.80 mM respectively which are comparable to the corresponding reports in literature (Umar et al., 2009; Matharu et al., 2012; Ahmadalinezhad and Chen, 2011). It is important to note that the detection process in present work occurs at very low potential (0.2 V). At such a low potential the effect of other electrochemically active species like ascorbic acid, uric acid etc. present in the biological samples would be almost negligible.

To study the effect on non-specific signal, various non-specific analytes (glucose (5 mM), uric acid (0.1 mM), urea (1 mM), Ascorbic acid (0.05 mM) and Lactic Acid (0.05 mM)) were added separately in the buffer solution along with along with the normal concentration (5.2 mM) of cholesterol and then the sensor response was measured. It was found that the non-specific analytes interfered only slightly with the sensor response towards the cholesterol. The maximum interference (less than 3%) was obtained for glucose. Thus the possible interference which could occur due to non-specific signals with the sensing response of analyte was within permissible limits.

The sensor is repeatable atleast upto 10 times. The experiment was carried out at different times and the sensor response was found to vary within $\pm$2% of the sensor response.

Extensive experiments were carried out over a span of one week under different ambient conditions. The measured sensor response for fixed concentration of analyte was found to vary insignificantly with various external conditions, thus the sensor is found to be robust.

To determine the shelf life of the prepared bioelectrodes, CV studies were carried out at regular interval of time over a span of 14 weeks. The magnitude of I_{po} obtained with each successive

Table 1
Determination and recovery of cholesterol in human serum samples.

Sample number	Concentration of Cholesterol (mM)			R.S.D. of developed biosensor ($n=4$) (%)	Spike (mM)	Data after spike		
	Prepared Total	Biosensor Free	Spectrophotometric method in Path Lab			Concentration of cholesterol using biosensor (mM)	Recovery (%)	R.S.D. of developed biosensor ($n=4$) (%)
1	2.24	0.71	2.32	1.8	5	7.21	99.4	1.4
2	3.12	0.92	3.16	2.1	5	8.27	103	1.9
3	4.24	1.14	4.15	1.6	5	9.04	99.6	2.1
4	5.09	1.52	5.17	2.1	5	10.36	104	2.2

week was compared with its initial value. Activity of bioelectrode was calculated in percentage using the obtained values of I_{po} after certain interval of time compared to its original value, and is shown in Supplementary Fig. S1(a). The shelf life studies of the prepared ChOx/(ZnO–CuO)/ITO/glass and (ChEt–ChOx)/(ZnO–CuO)/ITO/glass bioelectrode shows that the bioelectrodes based on composite matrix retain 90% activity even after 10 weeks, (Supplementary Fig. S1(a)), The high stability of bioelectrode in the present work may be attributed to preparation of highly stable composite thin film matrix of ZnO–CuO using the PLD technique.

3.10. Photometric assay

UV–visible spectroscopy has been used to study the photometric enzyme array of the prepared bioelectrodes and to estimate the enzyme activity. The ChOx/(ZnO–CuO)/ITO/glass and (ChEt–ChOx)/(ZnO–CuO)/ITO/glass bioelectrodes are dipped in 3 ml PBS solution containing 20 μl of HRP (1 mg/ml in PBS), 20 μl of o-dianisidine dye (1% in de-ionized water), and 100 μl of respective analyte (Cholesterol and total cholesterol) in different concentrations and is kept for about 3 min for incubation. The difference between the initial and final values of absorbance (Ab) measured at wavelength of 500 nm after 3 min of incubation of both bioelectrodes ChOx/(ZnO–CuO)/ITO/glass and (ChEt–ChOx)/(ZnO–CuO)/ITO/glass in the respective analyte solutions are obtained and shown in Supplementary Fig. S1(b) as a function of the concentration of respective analyte. The values of Ab was found to increase continuously with increase in analyte concentration for respective bioelectrodes. The apparent enzyme activity, i. e. the amount of enzyme bound on the surface of the prepared ZnO–CuO composite matrix, has been calculated using the equation, $a_{app}^{enz}(\mathrm{U\,cm^{-2}}) = AV/\varepsilon ts$ where A is the difference in absorbance before and after incubation, V is the total volume (3.17 $\mathrm{cm^3}$), ε is the millimolar extinction coefficient (7.5 for *o*-dianisidine at 500 nm), t is the reaction time (3 min) and s is the surface area (0.25 $\mathrm{cm^2}$) of the prepared bioelectrode. Estimated value of the apparent enzyme activity on the surface of ChOx/(ZnO–CuO)/ITO/glass and (ChEt–ChOx)/(ZnO–CuO)/ITO/glass bioelectrodes was about 3.4×10^{-2} U $\mathrm{cm^{-2}}$ and 3.2×10^{-2} U $\mathrm{cm^{-2}}$ respectively, which are higher than the corresponding results reported for cholesterol using metal oxide matrices (Singh et al., 2007; Solanki et al., 2009).

3.11. Analysis of serum samples

The concentration of free cholesterol and total cholesterol was estimated in serum samples using the respective bioelectrodes and the corresponding calibration curves (inset (a) of Figs. 4 and 5). To gauge the performance of the fabricated biosensor, the content of total cholesterol in the serum samples determined by the (ChEt–ChOx)/(ZnO–CuO)/ITO/glass biosensor was compared with the corresponding data obtained for the commercial spectrophotometric method. Table 1 summarizes the results obtained on the serum analysis. The results presented in Table 1 indicate that the total cholesterol analysis in serum with the developed biosensor is in good agreement with the spectrophotometric data. It is important to emphasize that the laboratory value of free cholesterol was not available but its value is approximately 30% of total cholesterol content in all the cases. Subsequently, the real samples were spiked with known concentration (5 mM) of total cholesterol and the recovery tests were performed using the fabricated biosensor (Table 1). The recovery tests reveal that the (ChEt–ChOx)/(ZnO–CuO)/ITO/glass biosensor is accurate and precise and hence its performance is comparable with the commrcially accepted methods.

4. Conclusion

An enzymatic reagentless biosensor for the detection of free and total cholesterol has been fabricated based on ZnO–CuO composite thin film matrix. Presence of CuO induces the desired redox property in the composite matrix along with improved electron communication feature. The ChOx/(ZnO–CuO)/ITO/glass and (ChEt–ChOx)/(ZnO–CuO)/ITO/glass bioelectrodes exhibits linear response for detection of free cholesterol and total cholesterol in the range of 0.12–12.93 mM and 0.5–12 mM respectively. The fabricated biosensors show excellent sensitivity of 680 μA $\mathrm{mM^{-1}}$ $\mathrm{cm^{-2}}$ and 760 μA $\mathrm{mM^{-1}}$ $\mathrm{cm^{-2}}$ for free cholesterol and total cholesterol respectively with relatively fast response time of 5 s. The results obtained on serum sample, in close agreement with the commercial spectroscopic data, confirm the potential of prepared ZnO–CuO composite matrix for fast and reliable detection of free and total cholesterol.

Acknowledgments

The authors are thankful to University Grants Commission (UGC) (Grant no. 36-252/2008 (SR)) and Department of Science and Technology (DST) (Grant no. IDP/IMD/2010/28) for the financial support to carry out the proposed work. One of the authors (NB) is also thankful to the Council of Scientific and Industrial Research (CSIR) (Grant no. 09/045 (0869)/2009-EMR-1), India for the research fellowship and Indian Council of Medical Research (ICMR) (Grant no. 3/2/TG-49/HRD-2014 (21)) for travel grant.

Appendix A. Supplementary materials

Supplementary data associated with this article can be found in the online version at http://dx.doi.org/10.1016/j.bios.2014.08.029.

References

Ahmadalinezhad, A., Chen, A., 2011. Biosens. Bioelectron. 26, 4508–4513.
Ali, A., Ansari, A.A., Kaushik, A., Solanki, P.R., Barik, A., Pandey, M.K., Malhotra, B.D., 2009. Mater. Lett. 63, 2473–2475.

Bongiovanni, C., Ferri, T., Poscia, A., Varalli, M., Santucci, R., Desideri, A., 2001. Bioelectrochemistry 54, 17–22.
Cao, S., Zhang, L., Chai, Y., Yuan, R., 2013. Biosens. Bioelectron. 42, 532–538.
Gu, B.X., Xu, C.X., Zhu, G.P., Liu, S.Q., Chen, L.Y., Li, X.S., 2009. J. Phys. Chem. B 113, 377.
Gupta, V., Bhattacharya, P., Yuzuk, Y.I., Sreenivas, K., Katiyar, R.S., 2006. J. Cryst. Growth 287, 39.
Jindal, K., Tomar, M., Gupta, V., 2012. Biosens. Bioelectron. 38, 11–18.
Kim, S.S., Lee, B.T., 2004. Thin Solid Films 446, 307–312.
Kontkanen, H., Tenkanen, M., Reinikainen, T., 2006. Enzyme Microb. Technol. 39, 265–273.
Matharu, Z., Solanki, P.R., Gupta, V., Malhotra, B.D., 2012. Analyst 137, 747.
Matharu, Z., Sumana, G., Arya, S.K., Singh, S.P., Gupta, V., Malhotra, B.D., 2007. Langmuir 23, 13188–13192.
Parlak, O., Tiwari, A., Turner, A.P.F., Tiwari, A., 2013. Biosens. Bioelectron. 49, 53–62.
Saha, S., Gupta, V., 2011a. J. Appl. Phys. 110, 064904.
Saha, S., Gupta, V., 2011b. AIP Adv. 1, 042112.
Singh, S.P., Arya, S.K., Pandey, P., Malhotra, B.D., Saha, S., Sreenivas, K., Gupta, V., 2007. Appl. Phys. Lett. 91, 063901.
Solanki, P.R., Kaushik, A., Ansari, A.A., Malhotra, B.D., 2009. Appl. Phys. Lett. 94, 143901.
Tsoutsouva, M.G., Panagopoulos, C.N., Papadimitriou, D., Fasaki, I., Kompitsas, M., 2011. Mater. Sci. Eng. B 176, 480–483.
Tyagi, M., Tomar, M., Gupta, V., 2012. Anal. Chim. Acta 726, 93–101.
Umar, A., Rahman, M.M., Al-Hajry, A., Hahn, Y.B., 2009. Talanta 78, 284–289.
Wang, Z., Yang, Y., Li, J., Gong, J., Shen, G., Yu, R., 2006. Talanta 69, 686.
Wei, X.Q., Zhang, Z., Yu, Y.X., Man, B.Y., 2009. Opt. Laser Technol. 41, 530–534.
Yadav, H.K., Sreenivas, K., Gupta, V., 2010. J. Appl. Phys. 107, 044507.
Yadav, H.K., Gupta, V., 2012. J. Appl. Phys. 111, 102809.
Zerdali, M., Hamzaoui, S., Teherani, F.H., Rogers, D., 2006. Mater. Lett. 60, 504–508.
Zhu, Y., Sow, C., Yu, T., Zhao, Q., Li, P., Shen, Z., Yu, D., Thong, J.T., 2006. Adv. Funct. Mater. 16, 2415–2422.
Zhu, X., Yuri, I., Gan, X., Suzuki, I., Li, G., 2007. Biosens. Bioelectron. 22, 1600.
Zhu, L., Xua, L., Tan, L., Tan, H., Yang, S., Yao, S., 2013. Talanta 106, 192–199.

Please cite this article as: Batra, N., et al., Biosensors and Bioelectronics (2014), http://dx.doi.org/10.1016/j.bios.2014.08.029